Sucrose non-fermenting 1-related kinase promotes angiogenesis *in vivo*

Qiulun Lu[1], **Zhonglin Xie**[1], **Chenghui Yan**[1], **Ye Ding**[1], **Zejun Ma**[1], **Shengnan Wu**[1], **Yu Qiu**[1], **Stephanie M. Cossette**[2], **Michelle Bordas**[2], **Ramani Ramchandran**[2,3,*], and **Ming-Hui Zou**[1,*]

[1]Center for Molecular and Translational Medicine, Georgia State University, Atlanta, GA

[2]Department of Pediatrics, Division of Neonatology, Medical College of Wisconsin, Milwaukee, WI

[3]OBGYN, Developmental Vascular Biology Program, Children's Research Institute, Medical College of Wisconsin, Milwaukee, WI

Abstract

Objective—Sucrose non-fermenting 1 (Snf1)-related kinase (SNRK) is a novel member of the AMP-activated protein kinase (AMPK)-related superfamily that is activated in the process of angiogenesis. Currently, little is known about the function of SNRK in angiogenesis in the physiological and pathological condition.

Approach and Results—In this study, in *Snrk* global heterozygous knockout mice, retina angiogenesis and neovessel formation after hindlimb ischemia were suppressed. Consistently, mice with EC-specific *Snrk* deletion exhibited impaired retina angiogenesis, and delayed perfusion recovery and exacerbated muscle apoptosis in ischemic hindlimbs, compared with those of littermate wide-type mice. Endothelial SNRK expression was increased in the extremity vessel samples from non-ischemic human. In endothelial cells (ECs) cultured in hypoxic conditions, hypoxia inducible factor 1α (HIF1α) bound to the *SNRK* promoter to upregulate *SNRK* expression. In the nuclei of hypoxic ECs, SNRK complexed with specificity protein 1 (SP1), and together, they bound to an SP1-binding motif in the β1 integrin (ITGB1) promoter, resulting in enhanced ITGB1 expression and promoted EC migration. Furthermore, *SNRK* or *SP1* deficiency in ECs ameliorated hypoxia-induced ITGB1 expression and, consequently, inhibited EC migration and angiogenesis.

Conclusions—Taken together, our data have revealed that SNRK/SP1-ITGB1 signaling axis promotes angiogenesis *in vivo*.

*Correspondence to Ming-Hui Zou, MD, PhD, Center for Molecular and Translational Medicine, Georgia State University, 157 Decatur Street SE, Atlanta, GA, 30303, USA; phone: 404-413-6637; fax: 404-413-3580; mzou@gsu.edu or Dr. Ramani Ramchandran, 8701 Watertown Plank Road; P.O. Box 26509 Milwaukee, WI 53226 Office: (Peds) 414-955-2387, (OBGYN) 414-805-4791, rramchan@mcw.edu.

Author contributions

M.Z and Z.X conceived the project. Q.L, Z.X, and M.H.Z designed experiments, analyzed the data, and wrote the manuscript. S.C., M.B., and R.R performed the experiments with Tie2-targeted SNAR mice, generated the mice, and revised the manuscript. Q.L, C.Y, D.Y, Z.M, M.B and S.W performed in part experiments and analyzed data. Y.Q, M.B helped to breed and to maintain mouse stains.

Disclosures

None

Keywords

SNRK; migration; angiogenesis

Introduction

Angiogenesis plays crucial roles in some physiological conditions including organogenesis and advanced embryonic development, and is also a key process in pathological conditions such as stroke, myocardial infarction, and other ischemic diseases. The major function of the circulatory system is to deliver oxygen and nutrients to all cells and remove waste products within the body.[1, 2] An insufficient blood supply, if not corrected in time, leads to depletion of oxygen and nutrients to vital organs, resulting in organ failure and death.[1, 3, 4]

In response to sub-lethal changes in blood or oxygen supply, mammals have developed several mechanisms during evolution to alleviate ischemic or hypoxic injury. One of these adaptive mechanisms is angiogenesis, a process in which new capillaries form from existing microvessels to restore tissue blood perfusion to ischemic tissues.[5, 6] Overwhelming evidence indicate that one of the most potent stimulators of ischemic angiogenesis is hypoxia or reduced oxygen.[7] Hypoxia promotes the release of multiple classic proangiogenic factors, including fibroblast growth factor, vascular endothelial growth factor (VEGF), and angiopoietin, and this response is reported to be essential for microvascular density increases.[8–12] Although hypoxia inducible factors (HIFs) are key regulators of these adaptive hypoxic responses, precisely how these HIF transcription factors promote compensatory angiogenesis is not well known. Moreover, the targets of HIF transcription factors in endothelial cells (ECs) remain to be identified.

Sucrose non-fermenting 1 (Snf1)-related kinase (SNRK) is a serine/threonine kinase and a novel member of the AMP-activated protein kinase (AMPK)-related superfamily.[13, 14] The catalytic domain of SNRK has significant homology with those of AMPK and AMPK-related kinase.[15–24] Similar to AMPK, SNRK can be phosphorylated by liver kinase B1 (LKB1) at the Thr 173 residue located in the T-loop domain,[15] and is activated by 5-aminoimidazole-4-carboxamide ribonucleotide (AICAR) and cellular stressors such as glucose deprivation, rotenone, and sorbitol.[25, 26] Recent evidence suggests that SNRK regulates critical cellular processes, including glucose transportation and cell motility.[25, 27] Meanwhile, SNRK can improved cardiac mitochondrial efficiency and decreases mitochondrial uncoupling through uncoupling protein 3 (UCP3) pathway.[28] What's more, SNRK is aberrantly expressed in human diseases such as cancer and obesity.[26, 29] The essential role of SNRK in development is best demonstrated by the fact that homozygous deletion of *Snrk* in mice is embryonically lethal.[30] Although SNRK has been shown to regulate angioblast development in zebrafish,[27, 31] it is not known whether SNRK participates in hypoxia-induced angiogenesis.

The aim of the present study was to elucidate the roles of SNRK in angiogenesis. Here we report that SNRK protein levels in aorta samples from hindlimb ischemia and non-ischemia human. The increase of SNRK expression was via the binding of SNRK promoter by upregulation of hypoxia inducible factor 1α (HIF1α). Furthermore, we found that hypoxia-

upregulated SNRK promoted endothelial angiogenesis by activating β1 integrin (ITGB1)-mediated EC migration. Our results reveal a novel role for SNRK in angiogenesis, and suggest that SNRK upregulation is a valid therapeutic target in preventing and treating ischemic diseases.

Methods

Materials and Methods are available in the online-only Data Supplement.

Results

Retina angiogenesis is delayed in *Snrk* heterozygous mice

SNRK protein and mRNA levels were detected in retina from postnatal $Snrk^{f/wt}/Cre^{CMV-/-}$ (wild-type) mice and $Snrk^{f/wt}/Cre^{CMV+/-}$ (*Snrk* heterozygous) mice, and aorta from adult wild-type and *Snrk* heterozygous mice (Figure 1A–1C). To explore the role of SNRK in angiogenesis, we firstly studied that retinal angiogenesis occurs during the early postnatal days. *Snrk* heterozygous mice displayed a significantly delay in retinal angiogenesis, reflected from the reduction of vascular diameter and vascularized area (Figure 1D and 1E).

Angiogenesis is suppressed in *Snrk* heterozygous mouse model of hindlimb ischemia

To further confirm the role of SNRK in angiogenesis, hindlimb ischemia model was used. The left-leg femoral arteries of 2 months old $Snrk^{f/wt}/Cre^{CMV-/-}$ (wild-type) mice and $Snrk^{f/wt}/Cre^{CMV+/-}$ (*Snrk* heterozygous) mice were ligated, and then, blood flow restoration was monitored at different time points. At 2 weeks after surgery, the blood flow ratio returned to 0.33 ± 0.09 in wild-type mice, whereas the blood flow ratio only recovered to 0.17 ± 0.05 in *Snrk* heterozygous mice, indicating an obvious impairement in perfusion recovery in *Snrk* heterozygous mice (Figure 1F and 1G).

We also evaluated angiogenesis by immunostaining vWF-positive cells in ischemic tissues. At 2 weeks after ischemia induction, there was a significant reduction in the number of vWF-positive capillaries surrounding the skeletal muscle fibers in *Snrk* heterozygous mice compared with $Snrk^{f/wt}/Cre^{CMV-/-}$ (wild-type) mice (Figure 1H and 1I).

Hindlimb ischemia increases SNRK expression in the vasculature of skeletal muscle

To further confirm the effects of hypoxia on SNRK, we examined SNRK expression in wild-type mice subjected to femoral artery ligation. Four weeks after ligation, SNRK expression was significantly increased at the protein ($P < 0.05$) and mRNA ($P < 0.05$) level in the gastrocnemius muscle of the ischemic limbs compared with those in the sham-treated, non-ischemic limbs (Figure IA–C in the online-only Data Supplement). Moreover, there appeared to be more SNRK-positive cells in ischemic tissues than in the non-ischemic counterparts (Figure ID in the online-only Data Supplement). Co-immunostaining of SNRK and the EC marker vWF showed that SNRK staining was mainly in the vWF-positive cells (Figure 1D). In our mouse model of hindlimb ischemia, SNRK levels were upregulated in the vasculature of skeletal muscles in response to ischemia.

In aorta tissues from human, SNRK expression was mainly in endothelial cells (Figure IE in the online-only Data Supplement). Interesting, SNRK expression was obviously increased and the increase of SNRK expression was mainly in endothelial cells (Figure IE in the online-only Data Supplement). Thus, both in clinic and our mouse model of hindlimb ischemia, SNRK levels were upregulated in the vasculature of skeletal muscles in response to hypoxia.

Retina angiogenesis is delayed in EC-specific deletion *Snrk* mice

To target SNRK expression in endothelial cells, EC-specific deletion of *Snrk* (*Snrk*$^{f/f}$/Cre$^{VE-Cadh+/-}$) were generated by crossing *Snrk*$^{f/f}$ mice with VE-cad-Cre transgenic mice. Vascular diameter, vascularized area, and branch points in retinal tissues from *Snrk*$^{f/f}$/Cre$^{VE-Cadh+/-}$ mice were significantly suppressed compared with *Snrk*$^{wt/wt}$/Cre$^{VE-Cadh+/-}$ mice (Figure 2A and 2B).

Endothelial *Snrk* deletion impairs perfusion recovery and angiogenesis in ischemic hindlimbs

To determine whether *Snrk* deficiency impairs ischemia-induced angiogenesis *in vivo*, the left-leg femoral arteries of 3 months old *Snrk*$^{f/f}$/Cre$^{VE-Cadh+/-}$and *Snrk*$^{wt/wt}$/Cre$^{VE-Cadh+/-}$ (WT) mice were ligated, and then, blood flow restoration was monitored at different time points. Before surgery, the ratio of the left-to-right leg blood flow was 1. Directly after surgery, the blood flow ratio dropped by 90% in both mouse groups (Figure 2C). At 4 weeks after surgery, the blood flow ratio returned to 0.8 in control mice, whereas the blood flow ratio only recovered to 0.35 in *Snrk*$^{f/f}$/Cre$^{VE-Cadh+/-}$ mice, demonstrating a marked impairment in perfusion recovery in *Snrk*$^{f/f}$/Cre$^{VE-Cadh+/-}$ mice (Figure 2C). We also performed similar hind limb ischemia studies on 6 months old male *Snrk*-Tie2 Cre endothelial conditional knockout mice (*Snrk*$^{f/f}$/Cre$^{tie2+/-}$), and observed similar results in that blood flow ratio never recovered in the mutant mice compared to WT mice (*Snrk*$^{f/WT}$/Cre$^{tie2-/-}$ or *Snrk*$^{f/f}$/Cre$^{tie2-/-}$) (Figure IIA and IIB in the online-only Data Supplement), and the baselines between the control and mutant mice were already different, and persisted until 21 days. These results suggests that SNRK's effect in mediating angiogenesis is endothelial cell autonomous.

We also evaluated angiogenesis by immunostaining vWF-positive cells in ischemic tissues. At 4 weeks after ischemia induction, there was a noticeable increase in the number of vWF-positive capillaries surrounding the skeletal muscle fibers (neovascularization) in control mice. However, the numbers of vWF-positive capillaries surrounding the skeletal muscle fibers were significantly reduced in the *Snrk*$^{f/f}$/Cre$^{VE-Cadh+/-}$ mice compared with those of the control mice (Figure 2E and 2F).

Consistent with these data, hindlimb ischemia increased skeleton muscular apoptosis in *Snrk*$^{f/f}$/Cre$^{VE-Cadh+/-}$ mice compared to that in WT mice, as assessed by the increase in cleaved poly ADP ribose polymerase (PARP) and caspase-3 levels (Figure 2G). Thus, endothelial *Snrk* deletion inhibits angiogenesis in ischemic skeletal muscle.

HIF1α mediates hypoxia-induced SNRK expression

Hypoxia is often thought of as being a pathological phenomenon, such as in ischemic tissues, while the mammalian embryo in fact develops in a low-oxygen environment.[32] Therefore, we next investigated whether and how hypoxia regulates SNRK expression in human umbilical vein endothelial cells (HUVECs). Hypoxia induced increases in SNRK protein (Figure 3A and 3B) and mRNA (Figure 3C) levels in a time-dependent manner, and concomitantly upregulated HIF1α expression.[33] Similarly, treatment of HUVECs with cobalt chloride (CoCl$_2$) increased the expression of SNRK and HIF1α (Figure 3D–3F).

To establish whether HIF1α is essential for SNRK upregulation, we performed siRNA-mediated knockdown of HIF1α and assessed the effects on SNRK levels in hypoxic conditions. Transfection of *HIF1a* siRNA, but not control siRNA, in HUVECs ablated the hypoxia-induced increases in SNRK protein and mRNA levels (Figure 3G–3I). Conversely, overexpression of HIF1α in HUVECs markedly increased SNRK protein and mRNA levels in normoxic conditions (Figure 2J and 2K). Interestingly, HIF2α knockdown in HUVECs did not alter SNRK protein and mRNA levels in hypoxic or normoxic conditions (Figure IIIA–IIIC in the online-only Data Supplement), suggesting that hypoxia-induced SNRK expression is HIF1α dependent.

Identification of the HIF1α-specific binding site in the *SNRK* promoter

To further define how HIF1α regulates SNRK, the consensus HIF1α-binding site sequence 5′-(A/G)CGTG-3′ was used to identify putative binding sites in the human *SNRK* gene. As expected, four putative binding sites were found in the human *SNRK* promoter, which are located at −843 bp, −592 bp, −584 bp, and −290 bp upstream of the transcription start site (Figure 3L). To determine which of these HIF1α-binding sites in the *SNRK* promoter are functional, we constructed a series of luciferase reporter plasmids containing different lengths of the *SNRK* promoter, including pGL3 (control), pGL-SNRK-200 (no putative binding sites), pGL-SNRK-400 (one putative binding site at −290 bp), pGL-SNRK-700 (three putative biding sites at −290, −584, and −592 bp), and pGL-SNRK-900 (all four putative binding sites) (Figure 3L). Next, luciferase activity assays were performed in the plasmid-transfected HUVECs, with or without hypoxia, for 8 h. All three plasmids containing the SNRK promoter regions with the putative HIF1α-binding sites (pGL-SNRK-400, pGL-SNRK-700, and pGL-SNRK-900) showed significantly higher luciferase activities than that of the plasmid containing the SNRK promoter region lacking the putative HIF1α-binding sites (pGL-SNRK-200) and that of the pGL3 control plasmid (Figure 3M). Taken together, these results indicate that the putative binding site at −290 bp in the *SNRK* promoter is the HIF1α-specific binding site.

To further validate this result, we deleted the putative binding site at −290 bp in the pGL-SNRK-700 and pGL-SNRK-900 plasmids. The luciferase activities of pGL-SNRK-900-and pGL-SNRK-700-   were sharply decreased by 60 ± 5.7% and 41 ± 4.6% compared with those of pGL-SNRK-900 and pGL-SNRK-700, respectively (Figure 3M), demonstrating that the −290 bp HIF1α-binding site was critical for *SNRK* promoter activity. Moreover, this HIF1α-specific binding site in the *SNRK* promoter is conserved in five mammalian species,

including human, chimp, rhesus, mouse, and rat (Figure 3N), further indicating its functional relevance.

We further tested whether hypoxia promotes HIF1α binding to the −290 bp site in HUVECs. Chromatin immunoprecipitation (ChIP) assays showed that HIF1α did not bind to the *SNRK* promoter under normoxic conditions; however, hypoxia dramatically increased HIF1α binding to the *SNRK* promoter, and this binding was inhibited by siRNA-mediated silencing of HIF1α (Figure 3O). Collectively, these results indicate that HIF1α is required for hypoxia-activated SNRK expression in ECs.

SNRK deficiency impairs hypoxia-induced lung vascular EC migration

Because previous data suggested that SNRK deficiency suppresses angiogenesis *in vivo*, we next assessed how SNRK regulates angiogenesis in isolated lung EC cultures. First, SNRK absence was confirmed in lung ECs isolated from $Snrk^{f/f}/Cre^{VE-Cadh+/−}$ mice by western blot analysis (Figure 4A).

In wound healing assays, lung ECs from $Snrk^{f/f}/Cre^{VE-Cadh+/−}$ mice exhibited impaired migration, in normoxic and hypoxic conditions, compared with that of ECs from $Snrk^{wt/wt}/Cre^{VE-Cadh+/−}$ (WT) littermates (Figure 4B and 4C). Similarly, fewer ECs from $Snrk^{f/f}/Cre^{VE-Cadh+/−}$ mice migrated across the membrane in transwell migration assays than ECs from control littermates (Figure 4D and 4E).

To assess the effects of SNRK on endothelial migration *ex vivo*, we assessed microvessel sprouting from aortic rings isolated from $EYFP^{f/f}/Snrk^{f/f}/Cre^{VE-Cadh+/−}$ and $EYFP^{f/f}/Snrk^{wt/wt}/Cre^{VE-Cadh+/−}$ mice. In the aortic rings from control mice, the microvessels sprouted from the cut edges of the aortic rings and formed a microvessel network (Figure 4F–4H). In contrast, in $EYFP^{f/f}/Snrk^{f/f}/Cre^{VE-Cadh+/−}$ mice, the aortic rings exhibited reduced microvessel sprouting and network formation, as evidenced by the reduction in microvessel numbers and lengths compared with those of the control group (Figure 4F–4H).

These results showed that SNRK deficiency impaired angiogenesis mainly resulting from migration. And then many genes involving with migration were measured by realtime PCR. There is no significant difference of the mRNA levels of the growth factors between lung endothelial cells from $Snrk^{f/f}/Cre^{VE-Cadh+/−}$ and $Snrk^{wt/wt}/Cre^{VE-Cadh+/−}$ (WT) mice, such as VEGF, FGF2, and PDGF. And the mRNA levels of β1 integrin (ITGB1) were significantly suppressed in endothelial cells from $Snrk^{f/f}/Cre^{VE-Cadh+/−}$ mice, while the mRNA levels of Col1a2, and Col2a1 were obviously increased compared with $Snrk^{wt/wt}/Cre^{VE-Cadh+/−}$ (WT) mice, indicating ITGB1 can be regulated by SNRK involving with migration (Figure 4I).

SNRK is essential for EC migration

To confirm SNRK induction in a hypoxic environment is essential for EC function, we determined the impact of altering SNRK levels on angiogenesis in HUVECs. In wound healing assays, *SNRK* knockdown inhibited HUVECs migration into the wounded areas in normoxic and hypoxic conditions (Figure IVA and IVB in the online-only Data Supplement), and in transwell assays, *SNRK* silencing significantly reduced the numbers of migrating ECs (Figure IVC and IVD in the online-only Data Supplement). Transfection of

SNRK siRNA, but not scramble siRNA, ablated tube formation in normoxic and hypoxic conditions, as measured by tube branching points and vessel numbers (Figure IVE–IVG in the online-only Data Supplement).

Consistent with these data, SNRK overexpression promoted EC migration into the wounded areas (Figure VA and VB in the online-only Data Supplement) and increased the numbers of migrating ECs (Figure VC and VD in the online-only Data Supplement). In HUVECs tube formation assays, SNRK overexpression significantly promoted tube formation (Figure VE–VG in the online-only Data Supplement). Figure VIA in the online-only Data Supplement showed that SNRK expression levels were increased after SNRK overexpression in aorta. Moreover, in aortic ring assays, SNRK overexpression increased microvessel numbers and lengths (Figure VIB–VID in the online-only Data Supplement), confirming that SNRK promoted microvessel network formation.

B1 integrin upregulation promotes migration in lung ECs from *Snrk*[f/f]/Cre[VE-Cadh+/−] mice

Because of the significant reduction of the mRNA level of β1 integrin in lung ECs from *Snrk*[f/f]/Cre[VE-Cadh+/−] mice (Figure 4B), playing an important role in controlling EC migration,[34] and the increase of β1 integrin expression in response to hypoxia,[35] we next confirm whether β1 integrin is involved in lung ECs from *Snrk*[f/f]/Cre[VE-Cadh+/−] mice. As expected, hypoxia increased ITGB1 protein and mRNA levels in lung ECs from *Snrk*[wt/wt]/Cre[VE-Cadh+/−] mice (Figure 5A–5C). Importantly, the increase of ITGB1 expression caused by hypoxia was abolished in lung ECs from *Snrk*[f/f]/Cre[VE-Cadh+/−] mice (Figure 5A–5C).

We further tested whether ITGB1 overexpression rescues the cell migration defects in SNRK-deficient lung vascular ECs. As expected, in wound healing assays, ITGB1 overexpression promoted the migration of WT lung ECs into the wounded areas, and importantly, ITGB1 overexpression normalized the migration of SNRK-deficient lung ECs into the wounded areas (Figure 5D and 5E). In addition, in transwell migration assays, ITGB1 overexpression increased the numbers of WT and SNRK-deficient ECs that migrated across the membranes (Figure 5F and 5G). The phosphorylation of FAK and Scr, as downregulation gene of ITGB1, was suppressed in SNRK-deficient ECs compared with lung ECs from WT mice (Figure 5H). And ITGB1 overexpression can suppress the reduction of FAK and p Src phosphorylation caused by SNRK deficiency (Figure 5H).

SNRK promotes HUVECs migration by ITGB1 upregulation

To further confirm that β1 integrin is involved in SNRK-induced EC migration, we next examined whether β1 integrin overexpression can rescue the migration defection caused by SNRK knockdown in HUVECs. As expected, hypoxia increased ITGB1 protein and mRNA levels in HUVECs (Figure VIIA–VIIC in the online-only Data Supplement). Importantly, transfection of SNRK siRNA, but not scramble siRNA, abolished hypoxia-upregulated ITGB1 in HUVECs (Figure VIIA–VIIC in the online-only Data Supplement). Moreover, ITGB1 overexpression abolished the inhibitory effects of SNRK siRNA on HUVECs migration in wound healing assays (Figure VIID and VIIE in the online-only Data Supplement), transwell migration assays (Figure VIIF and VIIG in the online-only Data

Supplement), and tube formation assays (Figure VIIH–VIIJ in the online-only Data Supplement).

ITGB1 silencing abolishes the enhanced migration of SNRK-overexpressing HUVECs

To further establish the essential role of ITGB1 in SNRK-induced EC migration, we next tested whether ITGB1 is required for the observed increase in migration of SNRK-overexpressing HUVECs (Figure VIII in the online-only Data Supplement). Indeed, selective *ITGB1* knockdown abolished the increased migration and wound closure of SNRK-overexpressing ECs in wound healing assays (Figure IXA and IXB in the online-only Data Supplement), and prevented the enhanced migration of SNRK-overexpressing ECs across transwell membranes (Figure IXC and IXD in the online-only Data Supplement). Moreover, *ITGB1* knockdown abrogated the enhanced tube formation of SNRK-overexpressing ECs (Figure IXE–IXG in the online-only Data Supplement).

SNRK affect EC adhesion through ITGB1 pathway

The focal adhesion protein paxillin is required for the directional migration of ECs. To further elucidate how SNRK regulates EC migration through ITGB1, we examined the effects of SNRK modulation on HUVEC adhesion. *SNRK* siRNA-treated cells exhibited a dramatic reduction in paxillin staining and focal adhesions, compared with those of scramble siRNA-treated cells, indicating that SNRK depletion reduces HUVEC adhesion (Figure IXH and IXI in the online-only Data Supplement). In contrast, ITGB1 overexpression increased the number of HUVEC focal adhesions in the siSNRK- and siScramble-treated cells (Figure XA and XB in the online-only Data Supplement). Taken together, these data suggest that ITGB1 mediates the effects of SNRK on EC migration via cell adhesion regulation.

Hypoxia increases the association between SNRK and SP1

Specificity protein 1 (SP1)-binding sites have been identified within the ITGB1 promoter, and they are required for regulating the promoter activity.[35] To determine whether SNRK interacts with SP1 to regulate *ITGB1* expression, we examined the subcellular distribution of SNRK and SP1 in HUVECs by immunofluorescence staining. Consistent with previous reports,[36] SP1 was mainly present in the nucleus. Notably, SNRK was also predominantly detected in the nucleus (Figure 6A). We hypothesized that SNRK interacts with SP1 to regulate *ITGB1* expression; thus, we investigated whether SNRK directly associates with SP1. Immunoprecipitation of SP1 followed by probing for SNRK or vice versa showed that SNRK does physically associate with SP1 (Figure 6B and Figure XIA in the online-only Data Supplement). Moreover, the interaction between SP1 and SNRK was further enhanced in hypoxic conditions (Figure 6C and Figure XIB in the online-only Data Supplement).

SNRK and SP1 coordinately regulate *ITGB1* expression

Thorough analysis of the *ITGB1* gene revealed two putative SP1-binding motifs in the human *ITGB1* promoter, which are located at −4467 bp and −3263 bp upstream of the transcription start site (Figure XIC in the online-only Data Supplement). Luciferase reporter plasmids containing different lengths of the *ITGB1* promoter were generated and transfected into HEK293 cells. SP1 or SNRK overexpression significantly increased the luciferase

activities of the pGL-ITGB1-3263 and pGL-ITGB1-4467 plasmids, which each contained the candidate −3263 bp SP1-binding motif (Figure XID in the online-only Data Supplement). However, these luciferase activities were significantly decreased after deletion of the −3263 bp motif, suggesting that SP1 recognizes and binds to the human *ITGB1* promoter at the −3263 bp motif (Figure XID in the online-only Data Supplement).

To assess whether an intact SNRK/SP1 complex is crucial for SP1 binding to the *ITGB1* promoter, we performed ChIP assays in SNRK-overexpression and SNRK-deficient conditions. In HUVECs, SNRK overexpression enhanced SP1 binding to the *ITGB1* promoter (Figure 6D). In contrast, in lung ECs, SNRK deficiency inhibited SP1 binding to the *ITGB1* promoter (Figure 6E).

We reasoned that SNRK and SP1 coordinately regulate *ITGB1* expression through binding to the *ITGB1* promoter at the SP1-binding site. To test this, we measured *ITGB1* expression after transfection of HUVECs with SNRK and/or SP1 plasmids. Transfection of the SNRK or SP1 plasmid alone slightly increased ITGB1 protein and mRNA levels, whereas transfection of the SNRK and SP1 plasmids together dramatically increased ITGB1 protein and mRNA levels (Figure XIIA–XIIC in the online-only Data Supplement). In addition, *SP1* silencing abrogated the increased ITGB1 expression (protein and mRNA) in SNRK-overexpressing HUVECs (Figure 6F–6H). Similarly, *SNRK* knockdown abolished the increased ITGB1 expression (protein and mRNA) in SP1-overexpressing HUVECs (Figure 6I–6K). Finally, under hypoxic conditions, knockdown of *SNRK* and *SP1*, individually and in combination, prevented hypoxia-enhanced ITGB1 expression (Figure 6L and 6M). These results support the notion that SNRK and SP1 form a complex that binds the *ITGB1* promoter and synergistically upregulates *ITGB1* expression.

Discussion

In this study we have discovered that in ECs, *HIF1α*-induced SNRK upregulated ITGB1 expression, promoted EC migration, and increased the formation of endothelial tube-like structures. Conversely, *SNRK* silencing impaired EC migration and tube formation. Moreover, endothelial *Snrk* deletion impaired new vessel formation both in physiological and pathological condition and exacerbated ischemic injury in hindlimb ischemia mouse model. Our results suggest that the SNRK/SP1-ITGB1 signaling axis is essential for angiogenesis *in vivo*.

There are several novel findings of this study. First, we uncovered SNRK is involved with angiogenesis both in physiological and pathological conditions. In the healthy condition, sprouting angiogenesis, one vital step in the development of the retinal vasculature, is characterized by sprouts with endothelial cells. And in ischemic diseases, sprouting of capillaries leads to an increase of their density, resulting from the depletion of oxygen and nutrients. It is considered that angiogenesis is to be initiated after tissue ischemia. In the procedures of physiological development, retinal angiogenesis is suppressed both in SNRK global heterozygous knockout mice (*Snrk*^f/wt^/Cre^CMV+/−^) and EC-specific *Snrk* knockout (*Snrk*^f/f^/Cre^VE-Cadh+/−^) mice. In pathological condition, endothelial SNRK expression was increased in aorta tissues from patients bear extremity vessel diseases, while ischemia

induced SNRK expression in endothelial cells in hindlimb ischemic mouse model. Consistent with this finding, SNRK is mainly expressed in fetal CD34^{+} hematopoietic progenitor cells.[27] Additionally, blood perfusion and endogenous angiogenesis were suppressed after femoral ligation in SNRK global heterozygous knockout mice. We also observed decreased angiogenesis in the ischemic skeletal muscles of endothelial *Snrk*-deleted mice. Mice with EC-specific *Snrk* knockout exhibited impaired angiogenesis and delayed perfusion recovery in ischemic hindlimbs when compared with those of their littermate controls. It is recently reported that cardiomyocyte-specific SNRK knockout mice also show cardiac metabolism and functional deficits, and SNRK can decrease mitochondrial uncoupling, resulting in the cardiac protection against ischemia/reperfusion injury.[27] Overall, our results suggest that SNRK plays an essential role of angiogenesis, and that ischemic induction of endothelial SNRK is a key compensative adaptation to alleviate ischemic injury.

Secondly, we established a novel pathway in which hypoxia activated a HIF1α-SNRK/SP1-ITGB1 axis in endothelial cells to promote angiogenesis and alleviate ischemic injury. Several lines of evidence suggest that this axis is essential for ischemic adaptations to reduce tissue injury. First, hypoxia/ischemia induced HIF1α expression and concomitantly upregulated SNRK mRNA and protein expression. *HIF1α* knockdown completely abolished hypoxia-induced SNRK expression, whereas HIF1α overexpression increased SNRK expression. Thus, SNRK appears to be a HIF1α target in response to hypoxia. Indeed, the *SNRK* promoter has a HIF1α regulatory consensus sequence, or HRE, and we showed that HIF1α bound to the HRE of the *SNRK* promoter and increased its transcriptional activity in hypoxic conditions.

A third important finding of the present study is the identification of ITGB1 as the key mediator of SNRK-enhanced EC migration and angiogenesis. We found that SNRK upregulated ITGB1 expression by forming a complex with SP1. This complex bound to the *ITGB1* promoter and increased its transcriptional activity. *SP1* or *SNRK* silencing reduced the binding of this complex to the *ITGB1* promoter. In luciferase activity assays, SNRK or SP1 overexpression increased, whereas *SNRK* or *SP1* knockdown suppressed, *ITGB1* promoter luciferase activity. Further, SNRK and SP1 combined overexpression dramatically increased, whereas *SNRK* or *SP1* silencing reduced, ITGB1 mRNA and protein expression. Importantly, ITGB1 overexpression rescued the inhibitory effects of *SNRK* knockdown on EC migration[27] and tube formation. Conversely, *ITGB1* knockdown abrogated the enhanced migration and tube formation of SNRK-overexpressing ECs. Together, these data suggest that SNRK promotes angiogenesis by activating ITGB1-mediated EC migration and adhesion. Interestingly, ITGB1 overexpression in endothelial precursor cells has been directly implicated in augmenting angiogenesis in ischemic legs.[37] Our data that SNRK is a key regulator of ischemic angiogenesis combined with ITGB1's role in promoting angiogenesis in ischemic conditions, and hypoxia-induced SNRK triggers induction of ITGB1 expression in ECs provides a direct mechanistic link between the two proteins in promoting ischemia-related angiogenesis vivo.

In conclusion, we showed that hypoxia induced SNRK expression via HIF1α upregulation. The increased SNRK interacted with SP1 to enhance ITGB1 expression, which in turn,

promoted EC migration and increased new vessel formation. Thus, our data revealed SNRK as a novel molecule promoting hypoxia-induced angiogenesis, indicating that SNRK is a potential therapeutic target to treat ischemic diseases and other diseases associated with angiogenesis.

Supplementary Material

Refer to Web version on PubMed Central for supplementary material.

Acknowledgments

Abbreviations

AICAR	5-aminoimidazole-4-carboxamide ribonucleotide
AMPK	AMP-activated protein kinase
ChIP	chromatin immunoprecipitation
Col1a2	collagen type I alpha 2 chain
Col2a1	collagen type II alpha 1 chain
Col3a1	collagen type III alpha 1 chain
EBM	endothelial basal medium
EC	endothelial cell
FAK	focal adhesion kinase
FGF2	fibroblast growth factor 2
HIF1α	hypoxia inducible factor 1α
HRE	hypoxia response element
HUVECs	human umbilical vein endothelial cells
ITGB1	β-1 integrin
LKB1	liver kinase B1
PARP	poly ADP ribose polymerase
PDGF	platelet-derived growth factor

RPE	Retinal pigment epithelium
SEM	Standard error of the mean
SNRK	sucrose non-fermenting 1 (Snf1)-related kinase
SP1	specificity protein 1
TIE2	TEK Receptor Tyrosine Kinase
UCP3	uncoupling protein 3
VEGF	vascular endothelial growth factor
WT	wild type

References

1. O'Donnell MJ, Chin SL, Rangarajan S, et al. Global and regional effects of potentially modifiable risk factors associated with acute stroke in 32 countries (INTERSTROKE): a case-control study. Lancet. 2016; 388(10046):761–775. [PubMed: 27431356]

2. Goyal M, Menon BK, van Zwam WH, et al. Endovascular thrombectomy after large-vessel ischaemic stroke: a meta-analysis of individual patient data from five randomised trials. Lancet. 2016; 387(10029):1723–1731. [PubMed: 26898852]

3. Vidal-Petiot E, Ford I, Greenlaw N, Ferrari R, Fox KM, Tardif JC, Tendera M, Tavazzi L, Bhatt DL, Steg PG. Cardiovascular event rates and mortality according to achieved systolic and diastolic blood pressure in patients with stable coronary artery disease: an international cohort study. Lancet. 2016; 388(10056):2142–2152. [PubMed: 27590221]

4. Tegn N, Abdelnoor M, Aaberge L, Endresen K, Smith P, Aakhus S, Gjertsen E, Dahl-Hofseth O, Ranhoff AH, Gullestad L, Bendz B. Invasive versus conservative strategy in patients aged 80 years or older with non-ST-elevation myocardial infarction or unstable angina pectoris (After Eighty study): an open-label randomised controlled trial. Lancet. 2016; 387(10023):1057–1065. [PubMed: 26794722]

5. Wu B, Zhang Z, Lui W, et al. Endocardial cells form the coronary arteries by angiogenesis through myocardial-endocardial VEGF signaling. Cell. 2012; 151(5):1083–1096. [PubMed: 23178125]

6. Gao E, Lei YH, Shang X, Huang ZM, Zuo L, Boucher M, Fan Q, Chuprun JK, Ma XL, Koch WJ. A novel and efficient model of coronary artery ligation and myocardial infarction in the mouse. Circulation Research. 2010; 107(12):1445–1453. [PubMed: 20966393]

7. Okuno Y, Nakamura-Ishizu A, Otsu K, Suda T, Kubota Y. Pathological neoangiogenesis depends on oxidative stress regulation by ATM. Nature Medicine. 2012; 18(8):1208–1216.

8. Kikuchi R, Nakamura K, MacLauchlan S, Ngo DT, Shimizu I, Fuster JJ. An antiangiogenic isoform of VEGF-A contributes to impaired vascularization in peripheral artery disease. Nature Medicine. 2014; 20(12):1464–1471.

9. Cao R, Brakenhielm E, Pawliuk R, Wariaro D, Post MJ, Wahlberg E, Leboulch P, Cao Y. Angiogenic synergism, vascular stability and improvement of hind-limb ischemia by a combination of PDGF-BB and FGF-2. Nature Medicine. 2003; 9(5):604–613.

10. Ferraro B, Cruz YL, Baldwin M, Coppola D, Heller R. Increased perfusion and angiogenesis in a hindlimb ischemia model with plasmid FGF-2 delivered by noninvasive electroporation. Gene Therapy. 2010; 17(6):763–769. [PubMed: 20393507]

11. Aviles RJ, Annex BH, Lederman RJ. Testing clinical therapeutic angiogenesis using basic fibroblast growth factor (FGF-2). British Journal of Pharmacology. 2003; 140(4):637–646. [PubMed: 14534147]

12. Tan X, Yan K, Ren M, Chen N, Li Y, Deng X, Wang L, Li R, Luo M, Liu Y, Liu Y, Wu J. Angiopoietin-2 impairs collateral artery growth associated with the suppression of the infiltration of macrophages in mouse hindlimb ischaemia. Journal Translational Medicine. 2016; 14(1):306.

13. Kertesz N, Samson J, Debacker C, Wu H, Labastie MC. Cloning and characterization of human and mouse SNRK sucrose non-fermenting protein (SNF-1)-related kinases. Gene. 2002; 294(1-2): 13–24. [PubMed: 12234663]

14. Ding Y, Zhang M, Zhang W, Lu Q, Cai Z, Song P, Okon IS, Xiao L, Zou MH. AMP-Activated Protein Kinase Alpha 2 Deletion Induces VSMC Phenotypic Switching and Reduces Features of Atherosclerotic Plaque Stability. Circulation Research. 2016; 119(6):718–730. [PubMed: 27439892]

15. Jaleel M, McBride A, Lizcano JM, Deak M, Toth R, Morrice NA, Alessi DR. Identification of the sucrose non-fermenting related kinase SNRK, as a novel LKB1 substrate. FEBS Letters. 2005; 579(6):1417–1423. [PubMed: 15733851]

16. Wang Q, Zhang M, Torres G, Wu S, Ouyang C, Xie Z, Zou MH. Metformin Suppresses Diabetes-Accelerated Atherosclerosis via the Inhibition of Drp1-Mediated Mitochondrial Fission. Diabetes. 2017; 66(1):193–205. [PubMed: 27737949]

17. Xie Z, Dong Y, Scholz R, Neumann D, Zou MH. Phosphorylation of LKB1 at serine 428 by protein kinase C-zeta is required for metformin-enhanced activation of the AMP-activated protein kinase in endothelial cells. Circulation. 2008; 117(7):952–962. [PubMed: 18250273]

18. Li KR, Zhang ZQ, Yao J, Zhao YX, Duan J, Cao C, Jiang Q. Ginsenoside Rg-1 protects retinal pigment epithelium (RPE) cells from cobalt chloride ($CoCl_2$) and hypoxia assaults. PLoS One. 2013; 8(12):e84171. [PubMed: 24386346]

19. Chen Z, Peng IC, Sun W, Su MI, Hsu PH, Fu Y, Zhu Y, DeFea K, Pan S, Tsai MD, Shyy JY. AMP-activated protein kinase functionally phosphorylates endothelial nitric oxide synthase Ser633. Circulation Research. 2009; 104(4):496–505. [PubMed: 19131647]

20. Zhu H, Zhang M, Liu Z, Xing J, Moriasi C, Dai X, Zou MH. AMP-Activated Protein Kinase α1 in macrophages promotes collateral remodeling and arteriogenesis in mice in vivo. Arteriosclerosis Thrombosis and Vascular Biology. 2016; 36(9):1868–1878.

21. MacArthur JW Jr, Purcell BP, Shudo Y, Cohen JE, Fairman A, Trubelja A, Patel J, Hsiao P, Yang E, Lloyd K, Hiesinger W, Atluri P, Burdick JA, Woo YJ. Sustained release of engineered stromal cell-derived factor 1-alpha from injectable hydrogels effectively recruits endothelial progenitor cells and preserves ventricular function after myocardial infarction. Circulation. 2013; 128(11 Suppl 1):S79–S86. [PubMed: 24030424]

22. Xie Z, Dong Y, Zhang J, Scholz R, Neumann D, Zou MH. Identification of the serine 307 of LKB1 as a novel phosphorylation site essential for its nucleocytoplasmic transport and endothelial cell angiogenesis. Molecular and Cellular Biology. 2009; 29(13):3582–3596. [PubMed: 19414597]

23. Okon IS, Coughlan KA, Zhang C, Moriasi C, Ding Y, Song P, Zhang W, Li G, Zou MH. Protein kinase LKB1 promotes RAB7-mediated neuropilin-1 degradation to inhibit angiogenesis. The Journal of Clinical Investigation. 2014; 124(10):4590–4602. [PubMed: 25180605]

24. Zhang W, Wang Q, Wu Y, Moriasi C, Liu Z, Dai X, Wang Q, Liu W, Yuan ZY, Zou MH. Endothelial cell-specific liver kinase B1 deletion causes endothelial dysfunction and hypertension in mice in vivo. Circulation. 2014; 129(13):1428–1439. [PubMed: 24637557]

25. Li Y, Nie Y, Helou Y, Ding G, Feng B, Xu G, Salomon A, Xu H. Identification of sucrose non-fermenting-related kinase (SNRK) as a suppressor of adipocyte inflammation. Diabetes. 2013; 62(7):2396–2409. [PubMed: 23520131]

26. Zhang W, Wang Q, Song P, Zou MH. Liver kinase b1 is required for white adipose tissue growth and differentiation. Diabetes. 2013; 62(7):2347–2358. [PubMed: 23396401]

27. Chun CZ, Kaur S, Samant GV, Wang L, Pramanik K, Garnaas MK, Li K, Field L, Mukhopadhyay D, Ramchandran R. Snrk-1 is involved in multiple steps of angioblast development and acts via notch signaling pathway in artery-vein specification in vertebrates. Blood. 2009; 113(5):1192–1199. [PubMed: 18723694]

28. Rines AK, Chang HC, Wu R, Sato T, Khechaduri A, Kouzu H, Shapiro J, Shang M, Burke MA, Jiang X, Chen C, Rawlings TA, Lopaschuk GD, Schumacker PT, Abel ED, Ardehali H, et al. Snf1-related kinase improves cardiac mitochondrial efficiency and decreases mitochondrial uncoupling. Nature Communication. 2017; 8:14095.

29. Rines AK, Burke MA, Fernandez RP, Volpert OV, Ardehali H. Snf1-related kinase inhibits colon cancer cell proliferation through calcyclin-binding protein-dependent reduction of beta-catenin. FASEB Journal. 2012; 26(11):4685–4695. [PubMed: 22874833]

30. Cossette SM, Gastonguay AJ, Bao X, et al. Sucrose non-fermenting related kinase enzyme is essential for cardiac metabolism. Biology Open. 2014; 4(1):48–61. [PubMed: 25505152]

31. Pramanik K, Chun CZ, Garnaas MK, Samant GV, Li K, Horswill MA, North PE, Ramchandran R. Dusp-5 and Snrk-1 coordinately function during vascular development and disease. Blood. 2009; 113(5):1184–1191. [PubMed: 18927432]

32. Gerald D, Berra E, Frapart YM, Chan DA, Giaccia AJ, Mansuy D, Pouyssegur J, Yaniv M, Mechta-Grigoriou F. JunD reduces tumor angiogenesis by protecting cells from oxidative stress. Cell. 2004; 118(6):781–794. [PubMed: 15369676]

33. Kwan W, Cortes M, Frost I, Esain V, Theodore LN, Liu SY, Budrow N, Goessling W, North TE. The Central Nervous System Regulates Embryonic HSPC Production via Stress-Responsive Glucocorticoid Receptor Signaling. Cell Stem Cell. 2016; 19(3):370–382. [PubMed: 27424782]

34. Carbonell WS, DeLay M, Jahangiri A, Park CC, Aghi MK. Beta1 integrin targeting potentiates antiangiogenic therapy and inhibits the growth of bevacizumab-resistant glioblastoma. Cancer Research. 2013; 73(10):3145–3154. [PubMed: 23644530]

35. McClellan MJ, Khasnis S, Wood CD, Palermo RD, Schlick SN, Kanhere AS, Jenner RG, West MJ. Downregulation of integrin receptor-signaling genes by Epstein-Barr virus EBNA 3C via promoter-proximal and -distal binding elements. Journal of Virology. 2012; 86(9):5165–5178. [PubMed: 22357270]

36. Beishline K, Kelly CM, Olofsson BA, Koduri S, Emrich J, Greenberg RA, Azizkhan-Clifford J. Sp1 facilitates DNA double-strand break repair through a nontranscriptional mechanism. Molecular and Cellular Biology. 2012; 32(18):3790–3799. [PubMed: 22826432]

37. Goto K, Takemura G, Takahashi T, et al. Intravenous Administration of Endothelial Colony-Forming Cells Overexpressing Integrin beta1 Augments Angiogenesis in Ischemic Legs. Stem Cells Translational Medicine. 2016; 5(2):218–226. [PubMed: 26702126]

Highlights

Angiogenesis plays crucial roles in some physiological conditions including organogenesis and advanced embryonic development, and is also a key process in pathological conditions such as stroke, myocardial infarction, and other ischemic diseases.

Our results show that the increase of endothelial SNRK expression in in aorta samples from hindlimb ischemia and non-ischemia human.

The increase of SNRK expression was via the binding of SNRK promoter by upregulation of hypoxia inducible factor 1α (HIF1α).

Our study suggests that hypoxia-upregulated SNRK promoted endothelial angiogenesis by activating β1 integrin (ITGB1)-mediated EC migration.

From a clinical point of view, enhancing the expression of SNRK favors angiogenesis in preventing and treating ischemic diseases.
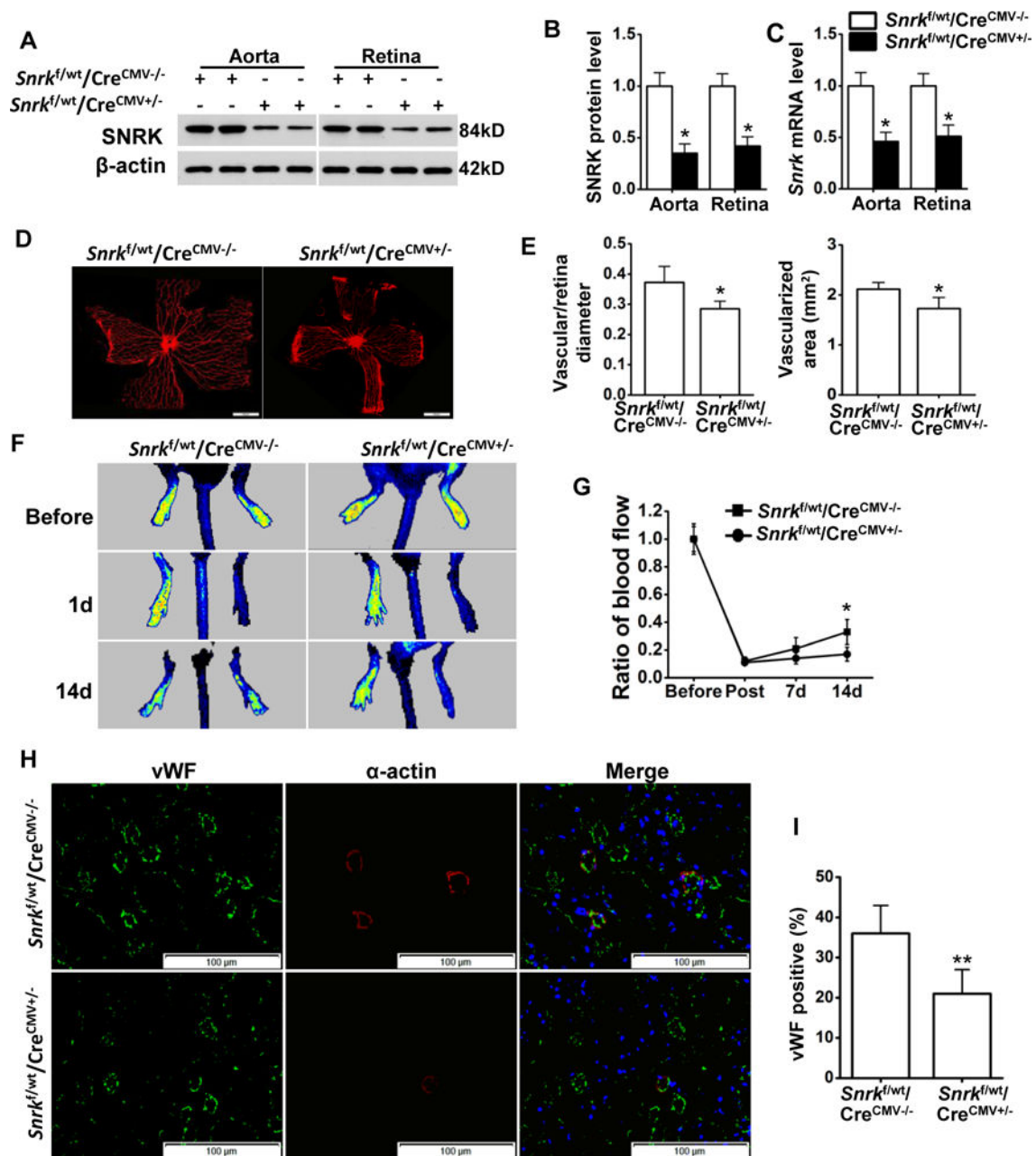
Figure 1. Delayed angiogenesis in *Snrk* heterozygous global knockout mouse

A-C, Aorta and retina tissues from *Snrk*^f/wt^/Cre^CMV−/−^ (wild-type) mice and *Snrk*^f/wt^/Cre^CMV+/−^ (*Snrk* heterozygous global knockout) mice. **B**, Densitometric analysis of the western blots (n = 6, * $P < 0.05$ vs. wild-type mice). **C**, mRNA levels of *Snrk* in aorta and retina tissues from wild-type mice and *Snrk* heterozygous global knockout mice (n = 6, * $P < 0.05$ vs. wild-type mice, *t*-test analysis). **D**, Isolectin B4 staining was analyzed in whole mounts of retinal vasculature in *Snrk*^f/wt^/Cre^CMV−/−^ and *Snrk*^f/wt^/Cre^CMV+/−^ mice. **E**, The bar graphs summarized isolectin B4 staining from 3 mice per group in each experiment and experiments were independently performed 3 times (* $P < 0.05$ vs. *Snrk*^f/wt^/Cre^CMV−/−^ mice, *t*-test analysis). **F**, Representative images show Laser Doppler Imaging analyses of hindlimb

blood perfusion in each group. Yellow indicates normal perfusion, whereas blue indicates a reduction in blood flow. **G**, Serial quantitative analysis was used to calculate the left (ischemic): right (normal) hindlimb perfusion ratios in $Snrk^{f/wt}/Cre^{CMV-/-}$ (wild-type) mice and $Snrk^{f/wt}/Cre^{CMV+/-}$ ($Snrk$ heterozygous global knockout) mice using Laser Doppler Imaging (n = 10/group, * $P < 0.05$ vs. $Snrk^{f/wt}/Cre^{CMV-/-}$ mice; ** $P < 0.01$ vs. $Snrk^{f/wt}/Cre^{CMV-/-}$ mice, t-test analysis). **H**, Immunofluorescent co-staining of vWF and α-actin in the gastrocnemius muscle from mice 2 weeks after femoral artery ligation. **I**, The immunofluorescent staining of vWF in the gastrocnemius muscle was quantitatively analyzed (n = 10/group, * $P < 0.05$ vs. $Snrk^{f/wt}/Cre^{CMV-/-}$ mice, t-test analysis).
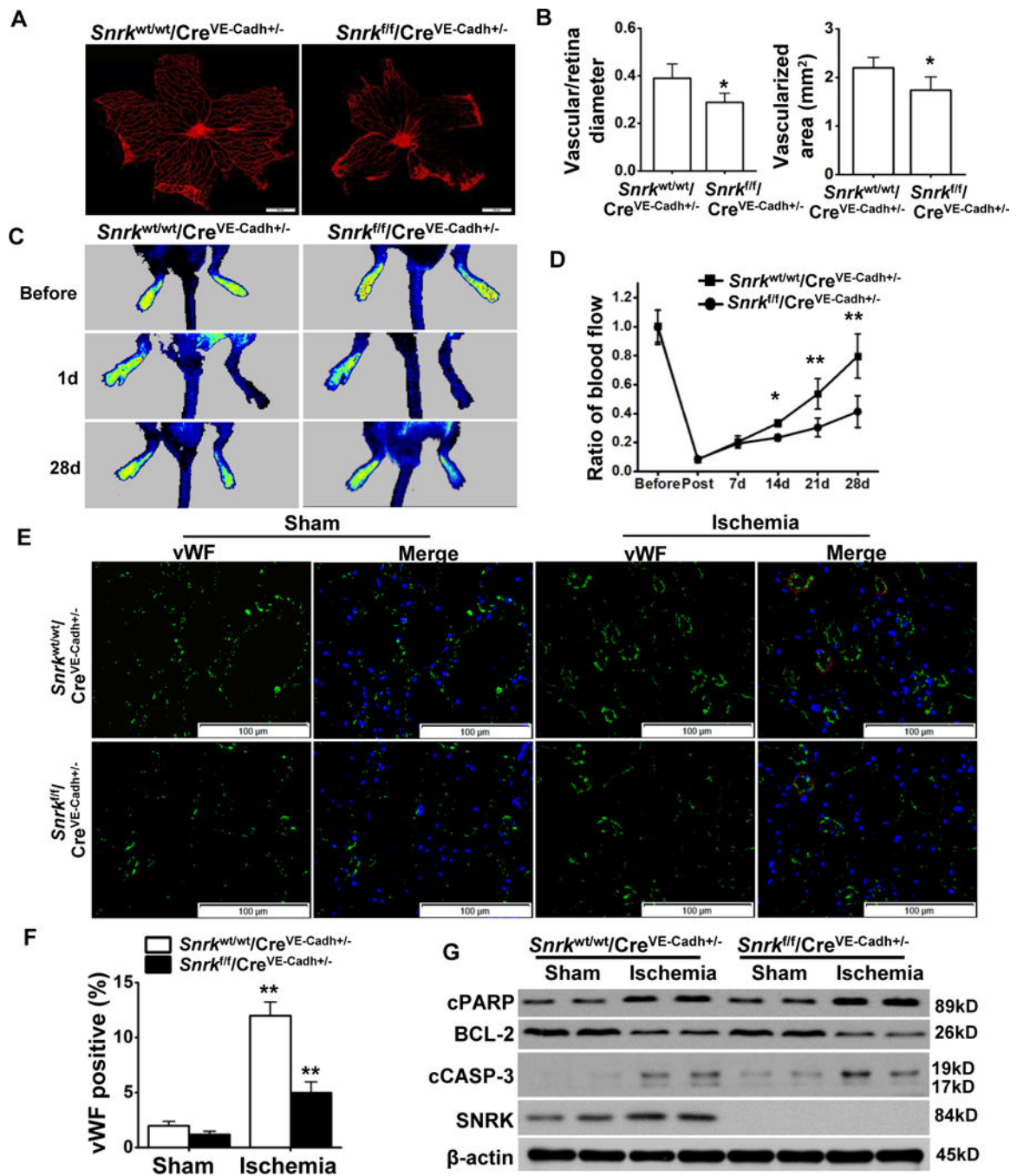
Figure 2. Angiogenesis is suppressed in endothelial cell-specific *Snrk* knockout mice
A, Isolectin B4 staining was analyzed in whole mounts of retinal vasculature in
Snrk^wt/wt^/Cre^VE-Cadh+/−^ (WT) and *Snrk*^f/f^/Cre^VE-Cadh+/−^ mice. **B**, The bar graphs
summarized isolectin B4 staining from 3 mice per group in each experiment and
experiments were independently performed 3 times (* $P < 0.05$ vs. *Snrk*^wt/wt^/Cre^VE-Cadh+/−^
mice, *t*-test analysis). **C**, Representative images show Laser Doppler Imaging analyses of
hindlimb blood perfusion in each group. Yellow indicates normal perfusion, whereas blue
indicates a reduction in blood flow. **D**, Serial quantitative analysis was used to calculate the

left (ischemic): right (normal) hindlimb perfusion ratios in $Snrk^{wt/wt}/Cre^{VE-Cadh+/-}$ (WT) and $Snrk^{f/f}/Cre^{VE-Cadh+/-}$ mice using Laser Doppler Imaging (n = 10/group, * $P < 0.05$ vs. $Snrk^{wt/wt}/Cre^{VE-Cadh+/-}$ mice; ** $P < 0.01$ vs. $Snrk^{wt/wt}/Cre^{VE-Cadh+/-}$ mice, t-test analysis at the each time point). **E**, Immunofluorescent co-staining of vWF and α-actin in the gastrocnemius muscle from mice 4 weeks after femoral artery ligation or sham surgery. **F**, The immunofluorescent staining of vWF in the gastrocnemius muscle was quantitatively analyzed. **G**, Endothelium-specific deletion of SNRK exacerbates ischemia-induced muscle apoptosis. Western blot analyses of apoptotic markers, including cleaved PARP (cPARP), cleaved Caspase-3 (cCASP-3), and BCL-2, in skeleton muscle tissues from $Snrk^{f/f}/Cre^{VE-Cadh+/-}$ and $Snrk^{wt/wt}/Cre^{VE-Cadh+/-}$ mice subjected to hindlimb ischemia or sham operation (n = 4, * $P < 0.05$ vs. $Snrk^{wt/wt}/Cre^{VE-Cadh+/-}$ sham. # $P < 0.05$ vs. $Snrk^{wt/wt}/Cre^{VE-Cadh+/-}$ ligation).
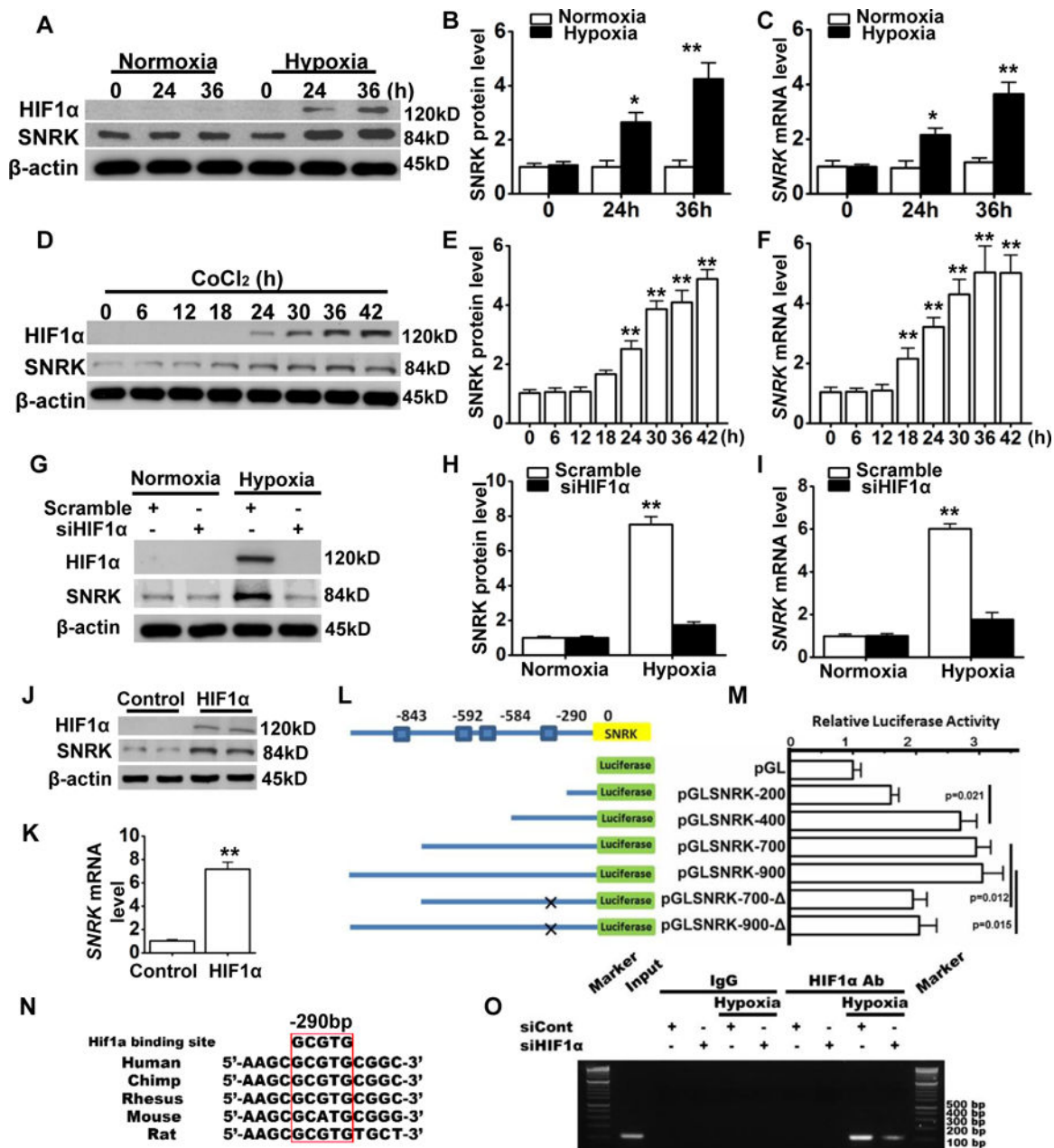
Figure 3. Hypoxia increases SNRK expression by upregulation of HIF1α in HUVECs

A, HUVECs were incubated in hypoxic conditions (1% O_2) for the indicated times, and the levels of SNRK, HIF1α, and β-actin were measured by western blotting. **B**, SNRK levels were quantified by densitometric analysis of the western blots (n = 6, * $P < 0.05$ vs. 0 h, *t*-test analysis). **C**, *SNRK* expression was measured by qRT-PCR (n = 6, * $P < 0.05$ vs. 0 h). **D**, HUVECs were treated with $CoCl_2$ (200 μmol/L) for the indicated times, and the protein levels of SNRK, HIF1α, and β-actin were measured by western blotting. **E**, SNRK levels were quantified by densitometric analysis of the western blots (n = 6, * $P < 0.05$ vs. 0 h, *t*-test analysis). **F**, *SNRK* expression was measured by qRT-PCR (n = 6, * $P < 0.05$ vs. 0 h). **G**, HUVECs were transfected with scramble or *HIF1α* siRNA (siHIF1α) for 48 h and then

treated with or without hypoxia (1% O_2) for 8 h. Cell lysates were subjected to western blot analysis to detect protein levels of SNRK, HIF1α, and β-actin. **H**, SNRK levels were quantified by densitometric analysis of the western blots (n = 6, * $P < 0.05$ vs. normoxia, *t*-test analysis). **I**, *SNRK* expression was measured by qRT-PCR (n = 6, * $P < 0.05$ vs. normoxia). **J**, HUVECs were transfected with HIF1α plasmid, and the levels of HIF1α and SNRK were measured by western blotting. **K**, *SNRK* mRNA expression was detected by qRT-PCR (n = 6, * $P < 0.05$ vs. control). **L**, A schematic representation illustrates the putative HIF1α-binding sites in the *SNRK* promoter and the reporter constructs used in the luciferase activity assays. **M**, For the *SNRK* promoter reporter assays, the transfected HUVECs were treated with hypoxia (1% O_2) for 8 h. The luciferase activities of the *SNRK* promoter deletion constructs are expressed as fold increases of the signal obtained with the plasmid containing the full-length promoter without hypoxia treatment. **N**, The hypoxia response element (HRE) motif (XCGTG) in the *SNRK* promoter, which is located at −290 bp upstream of the transcription start site, is conserved among five mammalian species. **O**, ChIP assays were performed to analyze the interaction between HIF1α and the *SNRK* promoter. HUVECs were incubated in hypoxic conditions for 8 h, and the chromatin was immunoprecipitated with an antibody against HIF1α. Rabbit IgG was used as a negative control. Precipitated DNA or 10% of the chromatin input were analyzed by PCR to amplify a 109-bp product containing the −290 bp HRE.
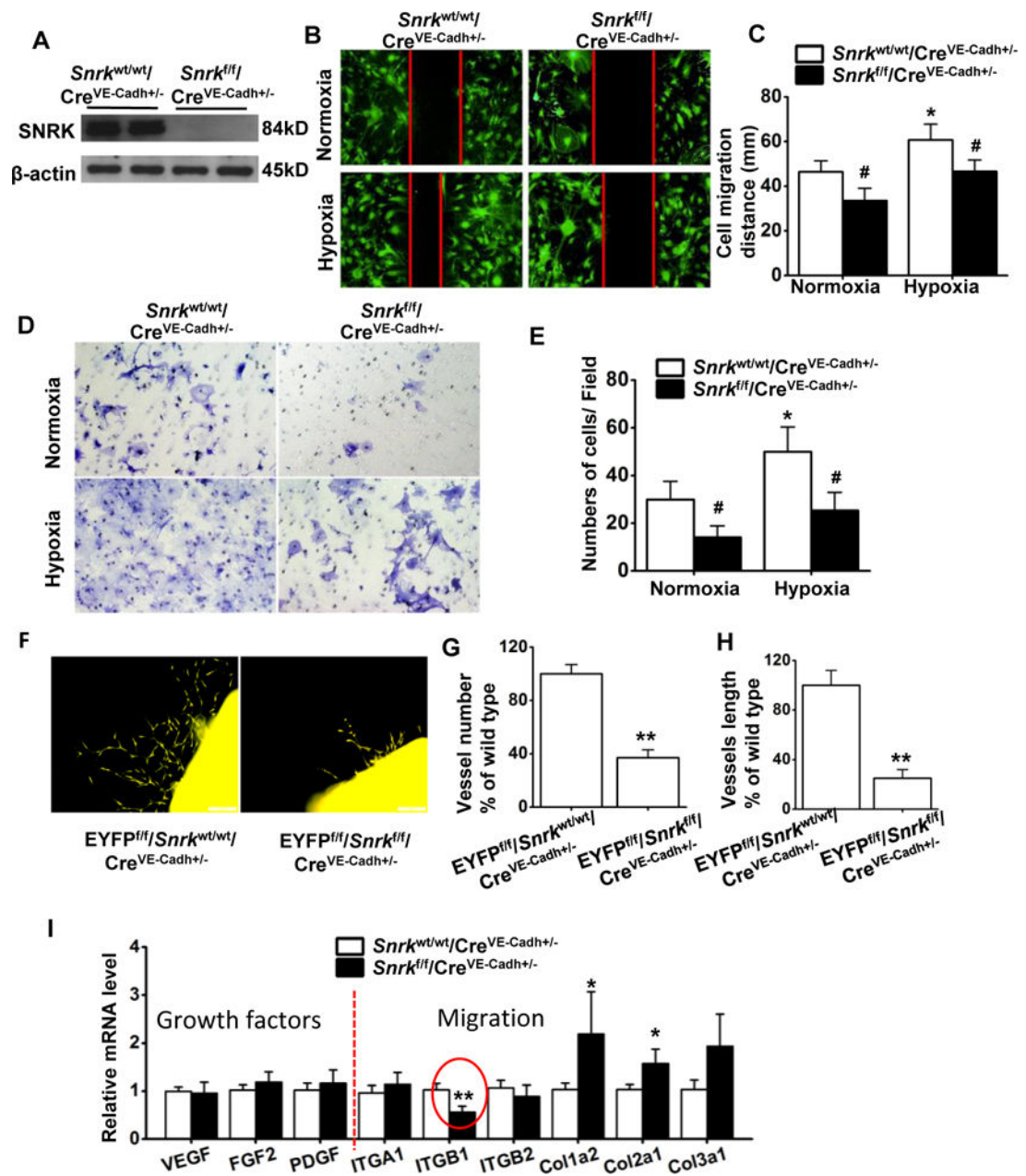
Figure 4. Migration is prevented in *Snrk*-deficient lung endothelial cells

A-F, Lung endothelial cells were isolated from *Snrk*$^{wt/wt}$/Cre$^{VE-Cadh+/-}$ (WT) and *Snrk*$^{f/f}$/Cre$^{VE-Cadh+/-}$ mice. **A**, Western blot analysis of Snrk protein levels in lung vascular endothelial cells from *Snrk*$^{wt/wt}$/Cre$^{VE-Cadh+/-}$ (WT) and *Snrk*$^{f/f}$/Cre$^{VE-Cadh+/-}$ mice. **B**, Representative images of lung endothelial cell migration in wound healing assay. **C**, Migration distances of lung endothelial cells (n = 4, * *P* < 0.05 vs. normoxia. # *P* < 0.05 vs. *Snrk*$^{wt/wt}$/Cre$^{VE-Cadh+/-}$ mice, *t*-test analysis). **D**, Lung endothelial cell migration was determined by transwell migration assays. **E**, Migrated cells were quantified (n = 4, * *P* < 0.05 vs. normoxia. # *P* < 0.05 vs. *Snrk*$^{wt/wt}$/Cre$^{VE-Cadh+/-}$ mice, *t*-test analysis). **F-H**, Aortic rings were prepared from EYFP$^{f/f}$/*Snrk*$^{wt/wt}$/Cre$^{VE-Cadh+/-}$ and EYFP$^{f/f}$/*Snrk*$^{f/f}$/

Cre$^{VE-Cadh+/-}$ mice, embedded in Matrigel, and cultured in growth medium for 6 days. **F,** Representative images show the neovessel formation from aortic rings embedded in Matrigel. Quantitative analyses of microvessel number **(G)** and length **(H)** for each genotype (n = 10, * $P < 0.05$ vs. EYFP$^{f/f}$/*Snrk*$^{wt/wt}$/Cre$^{VE-Cadh+/-}$, *t*-test analysis). **I,** Different gene expressions were measured by qRT-PCR in lung endothelial cells from WT and *Snrk*$^{f/f}$/Cre$^{VE-Cadh+/-}$ mice. (n = 6, * $P < 0.05$ vs. WT mice, ** $P < 0.01$ vs. WT mice).
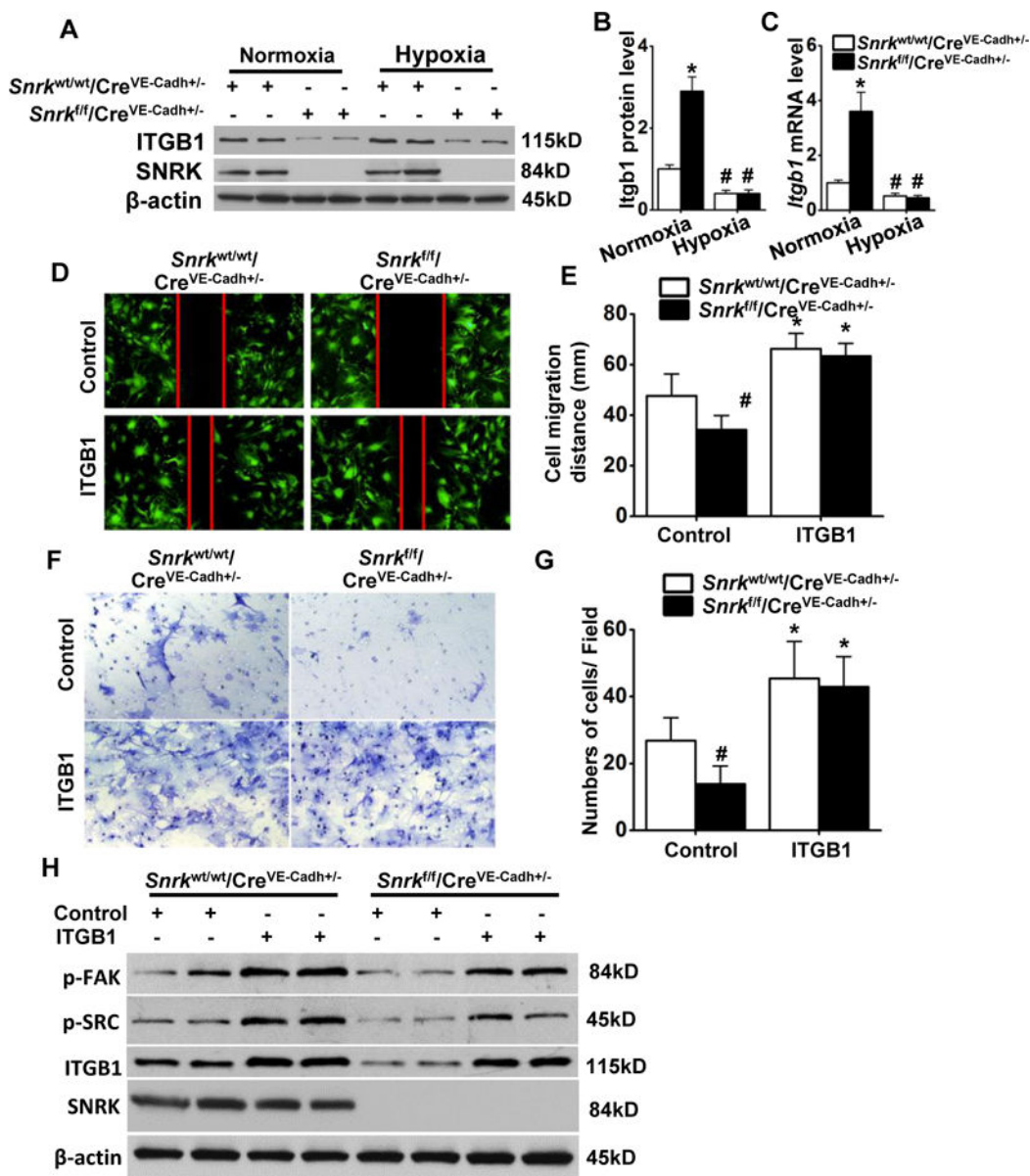
Figure 5. ITGB1 overexpression recovers cell migration in *Snrk*-deficient lung vascular endothelial cells

A, *Snrk*^f/f^/Cre^VE-Cadh+/−^ and *Snrk*^wt/wt^/Cre^VE-Cadh+/−^ lung vascular endothelial cells were treated with or without hypoxia (1% O$_2$) for 8 h. Cell lysates were subjected to western blot analysis to detect the levels of SNRK, ITGB1, and β-actin. **B**, Itgb1 levels were quantified by densitometric analysis of the western blots (n = 6, * $P < 0.05$ vs. *Snrk*^wt/wt^/Cre^VE-Cadh+/−^ lung vascular endothelial cells; # $P < 0.05$ vs. normoxia, *t*-test analysis). **C**, *Itgb1* expression was measured by qRT-PCR (n = 6, * $P < 0.05$ vs. *Snrk*^wt/wt^/Cre^VE-Cadh+/−^ lung vascular endothelial cells; # $P < 0.05$ vs. normoxia, *t*-test analysis). **D-H**, *Snrk*^f/f^/Cre^VE-Cadh+/−^ and *Snrk*^wt/wt^/Cre^VE-Cadh+/−^ lung vascular endothelial cells were transfected with control or ITGB1 plasmid for 48 h. **D**, Cell migration was examined by wound healing assay. **E**, Migration distances of HUVECs (*n* = 4, * $P < 0.05$ vs. control plasmid. # $P < 0.05$ vs.

Snrk^{wt/wt}/Cre^{VE-Cadh+/−}, *t*-test analysis). **F**, Cell migration was determined by transwell migration assay. **G**, Migrated cells were quantified ($n = 4$, * $P < 0.05$ vs. control plasmid. # $P < 0.05$ vs. *Snrk*^{wt/wt}/Cre^{VE-Cadh+/−}, *t*-test analysis). **H**, Cell lysates were subjected to western blot analysis to detect the levels of SNRK, ITGB1, p-FAK, p-SRC, and β-actin.

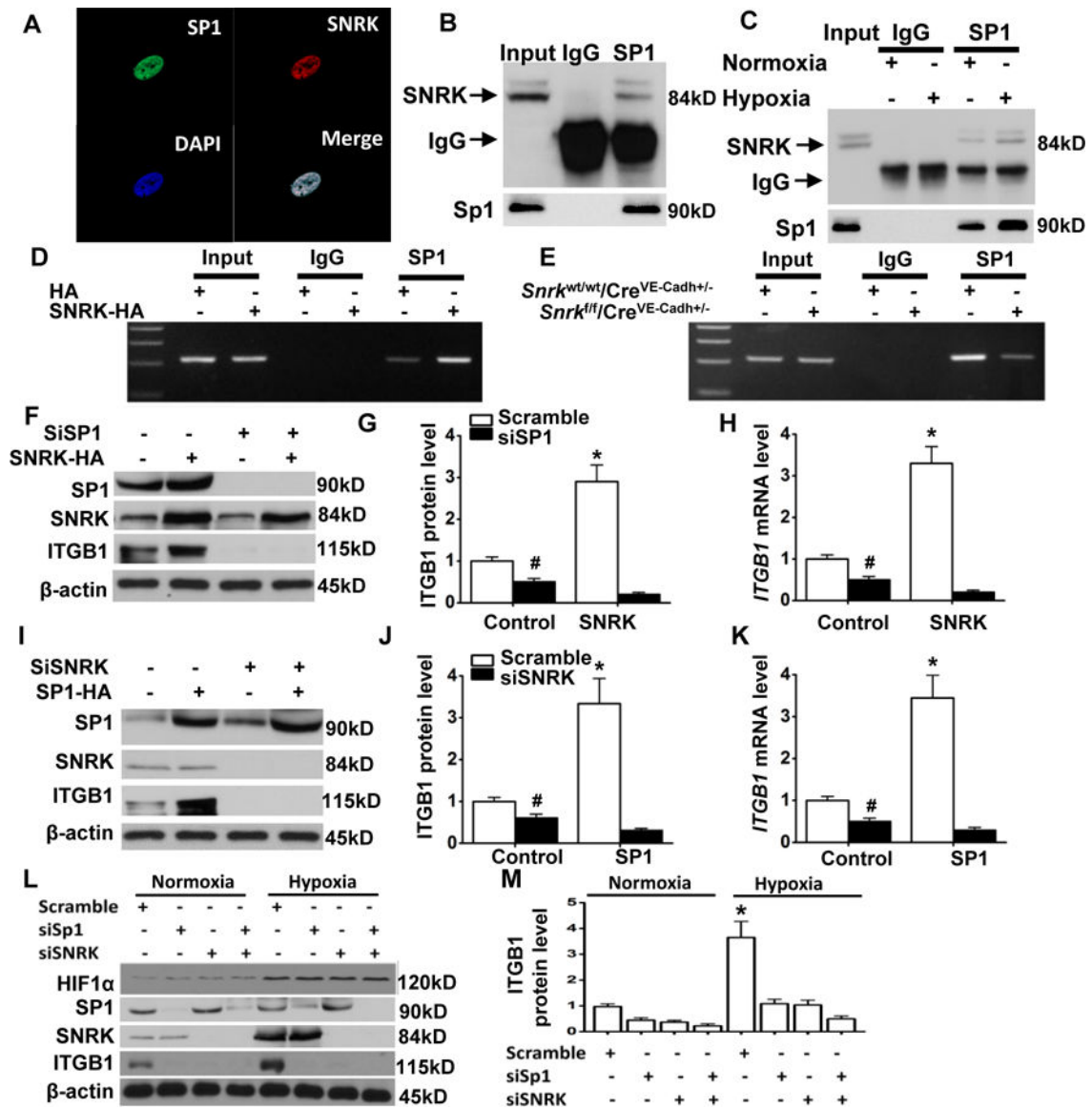*Snrk*$^{\text{wt/wt}}$/Cre$^{\text{VE-Cadh+/−}}$, *t*-test analysis). **F**, Cell migration was determined by transwell migration assay. **G**, Migrated cells were quantified ($n = 4$, * $P < 0.05$ vs. control plasmid. # $P < 0.05$ vs. *Snrk*$^{\text{wt/wt}}$/Cre$^{\text{VE-Cadh+/−}}$, *t*-test analysis). **H**, Cell lysates were subjected to western blot analysis to detect the levels of SNRK, ITGB1, p-FAK, p-SRC, and β-actin.

Figure 6. SNRK and SP1 coordinately regulate *ITGB1* expression
A, The subcellular distribution of SNRK and SP1 in HUVECs was examined by immunofluorescence staining. **B**, HUVEC lysates were immunoprecipitated with a SP1 antibody, and the immunoprecipitates were subjected to western blotting with a SNRK antibody (input: total cell lysates; IgG: immunoprecipitated with IgG). **C**, HUVECs were treated with or without hypoxia, and the interaction between SNRK and SP1 was analyzed by immunoprecipitation and western blotting (input: total cell lysates; IgG: immunoprecipitated with IgG). **D** and **E**, Chromatin was isolated from HUVECs transfected with plasmid encoding HA or SNRK-HA for 48 h (**D**) and from ECs isolated from *Snrk*^wt/wt^/Cre^VE-Cadh+/−^ or *Snrk*^f/f^/Cre^VE-Cadh+/−^ mice (**E**). The chromatin was immunoprecipitated with a SP1 antibody. Rabbit IgG was used as a negative control. A 210 bp product containing the SP1-binding site was amplified by PCR from immunoprecipitated DNA or 10% of the chromatin input. **F-H**, HUVECs were transfected with *SP1* siRNA and

SNRK-HA plasmid for 48 h. **F**, Cell lysates were subjected to western blot analysis to detect the levels of SP1, SNRK, ITGB1, and β-actin. **G**, ITGB1 levels were quantified by densitometric analysis of the western blots (n = 6, * $P < 0.05$ vs. control; # $P < 0.05$ vs. scramble siRNA, *t*-test analysis). **H**, *ITGB1* expression was measured by qRT-PCR (n = 6, * $P < 0.05$ vs. control; # $P < 0.05$ vs. scramble siRNA, *t*-test analysis). **I-K**, HUVECs were transfected with *SNRK* siRNA and SP1-HA plasmid for 48 h. **I)** Cell lysates were subjected to western blot analysis to detect the levels of SP1, SNRK, ITGB1, and β-actin. **J**, ITGB1 levels were quantified by densitometric analysis of the western blots (n = 6, * $P < 0.05$ vs. control; # $P < 0.05$ vs. scramble siRNA, *t*-test analysis). **K**, *ITGB1* expression was measured by qRT-PCR (n = 6, * $P < 0.05$ vs. control; # $P < 0.05$ vs. scramble siRNA, *t*-test analysis). **L** and **M**, HUVECs were co-transfected with *SP1*, *SNRK*, and scramble siRNAs, in various combinations, for 48 h in normoxic or hypoxic conditions. **L**, The levels of HIF1α, SP1, SNRK, ITGB1, and β-actin were measured by western blotting. **M**, ITGB1 levels were quantified by densitometric analysis of the western blots (n = 3, * $P < 0.05$ vs. normoxia, *t*-test analysis).